Radiation Measurements 93 (2016) 28–34

Contents lists available at ScienceDirect

Radiation Measurements

journal homepage: www.elsevier.com/locate/radmeas

The influence of field size and off-axis distance on photoneutron spectra of the 18 MV Siemens Oncor linear accelerator beam

Hrvoje Brkić [a], Ana Ivković [a, b], Mladen Kasabašić [a, b], Marina Poje Sovilj [c], Slaven Jurković [d, e], Damir Štimac [a, b], Otmar Rubin [a, b], Dario Faj [a, *]

[a] Faculty of Medicine Osijek, University of J.J. Strossmayer, Osijek, Croatia
[b] University Hospital Centre of Osijek, Osijek, Croatia
[c] Physics Department, University of J.J. Strossmayer Osijek, Osijek, Croatia
[d] University Hospital Centre of Rijeka, Rijeka, Croatia
[e] Medical Faculty Rijeka, University of Rijeka, Rijeka, Croatia

HIGHLIGHTS

- A model of medical linear accelerator (Siemens ONCOR) was built using the MCNP611 code.
- Neutron dose equivalent and energy spectrum in the patient plane was analyzed.
- Neutron flux increases with field size.
- Field size has almost no effect on the shape of neutron dose profiles.
- The mean energy of the neutrons increases with collimator opening at isocenter.

ARTICLE INFO

Article history:
Received 14 March 2016
Accepted 8 July 2016
Available online 12 July 2016

Keywords:
Radiotherapy
Neutron contamination
Monte Carlo

ABSTRACT

At present, high energy electron linear accelerators (LINACs) producing photons with energies higher than 10 MeV have a wide use in radiotherapy (RT). However, in these beams fast neutrons could be generated, which results in undesired contamination of the therapeutic beams. These neutrons affect the shielding requirements in RT rooms and also increase the out-of-field radiation dose to patients. The neutron flux becomes even more important when high numbers of monitor units are used, as in the intensity modulated radiotherapy. Herein, to evaluate the exposure of patients and medical personnel, it is important to determine the full radiation field correctly. A model of the dual photon beam medical LINAC, Siemens ONCOR, used at the University Hospital Centre of Osijek was built using the MCNP611 code. We tuned the model according to measured photon percentage depth dose curves and profiles. Only 18 MV photon beams were modeled. The dependence of neutron dose equivalent and energy spectrum on field size and off-axis distance in the patient plane was analyzed. The neutron source strength (Q) defined as a number of neutrons coming from the head of the treatment unit per x-ray dose (Gy) delivered at the isocenter was calculated and found to be 1.12×10^{12} neutrons per photon Gy at isocenter. The simulation showed that the neutron flux increases with increasing field size but field size has almost no effect on the shape of neutron dose profiles. The calculated neutron dose equivalent of different field sizes was between 1 and 3 mSv per photon Gy at isocenter. The mean energy changed from 0.21 MeV to 0.63 MeV with collimator opening from 0×0 cm^2 to 40×40 cm^2. At the 50 cm off-axis the change was less pronounced. According to the results, it is reasonable to conclude that the neutron dose equivalent to the patient is proportional to the photon beam-on time as suggested before. Since the beam-on time is much higher when advanced radiotherapy techniques are used to fulfill high conformity demands, this makes the neutron flux determination even more important. We also showed that the neutron energy in the patient plane significantly changes with field size. This can introduce significant uncertainty in dosimetry of neutrons due to strong dependence of the neutron detector response on the neutron energy in the interval 0.1–5 MeV.

* Corresponding author.
E-mail address: dariofaj@mefos.hr (D. Faj).

http://dx.doi.org/10.1016/j.radmeas.2016.07.002

1. Introduction

At present, high energy electron linear accelerators (LINACs) producing photons with energies higher than 10 MeV have a wide use in radiotherapy (RT). However, in these beams fast neutrons could be generated which results in undesired contamination of the therapeutic beams (NCRP60, 1984; Poje et al., 2014; Schraube et al., 2002; Vukovic et al., 2010). These neutrons affect the shielding requirements in RT rooms (Donadille et al., 2008) and also increase the out-of-field radiation dose to patients (McGinley et al., 1976; Naseri and Mesbahi, 2010). The neutron flux becomes more important when high numbers of monitor units (MU) are used as in the intensity modulated radiotherapy (IMRT) (Becker et al., 2008). Even more, all modern RT modalities aim to be highly conformal, what is achieved by using small fields and consequently requiring longer beam-on times. The beam-on time is proportional to the additional dose due to photoneutrons (Howell et al., 2005). Herein, it is important to determine the full radiation field correctly in order to evaluate the exposure of patients and medical personnel.

In this paper we present the Monte-Carlo (MC) simulation of LINAC Siemens Oncor 18 MV photon beams and neutron contamination in the patient plane in order to confirm that neutrons are significant contributor of the patient dose outside of treatment field (Kry et al., 2007; Ongaro et al., 2000). We will calculate dependence of neutron dose equivalent of field size and off-axis distance in the patient plane. The same data acquired by measurements are already presented (Jahangiri et al., 2015; Kry et al., 2005), but neutron dosimetry in mixed fields is still a very complex discipline where the most accurate techniques cannot achieve an uncertainty less than 10% (Chibani and Ma, 2003). This uncertainties are mainly due to saturation of neutron detectors by the photon flux and also due to the strong dependence of the neutron detector response on the neutron energy in the interval 0.1–5 MeV(Chibani and Ma, 2003; Zabihinpoor and Hasheminia, 2011). Consequently, it is important to know the neutron spectrum which contaminates the therapeutic photon beam to better evaluate the increase to the patient dose due to the neutron contamination.

It is well known that the neutrons originating from different parts of LINAC have different energies (Chen et al., 2006; Howell et al., 2005; Zanini et al., 2004). Consequently, it is reasonable to assume that there will be a neutron energy shift if neutrons produced by different parts of the LINAC head come to the measuring point in the patient plane. We assume that this will happen either when the field size is changed or when different points in a patient plane are chosen. Using MC simulations we will evaluate which part of the LINAC head produces neutrons coming to the chosen point in the patient plane if the field size or the measurement point in the patient plane is changed. The consequent energy change of photoneutrons in these situations will be calculated in order to minimize the uncertainty when neutron contamination in the patient plane is determined by measurements.

2. Materials and methods

The model of dual photon beam medical LINAC, Siemens ONCOR, used at University Hospital Centre of Osijek was built using MCNP611 code (Cox and Casswell, 2014). Nevertheless, due to negligible cross sections for neutron productions in a low energy photon beam (6 MV), only the high energy photon beam (18 MV) was modeled. To construct geometry that was defined in manufacturer's primer the model consisted of planes, cylinders and cones (Fig. 1). Materials defining the accelerator's head (its density and chemical structure) were also defined according to the manufacturer. The target was built in layers of stainless steel, tungsten, copper, aluminum, gold and nickel. The primary collimator (PC) and the jaws were made of tungsten, and the monitor chamber and the exit window of ceramic and glass, respectively. The surrounding space was filled with air of density 0.001293 g/cm^3.

Since the geometry of the flattening filter (FF) is not well defined in the primer, we constructed the geometry of the 18 MV FF according to the previously published data by Jabbari et al. (2013), with only slight geometrical modifications in order to fit our experimental data. Physical parameters of the original electron beam that may influence the dose profile and the central-axis percentage depth dose (PDD) curve are the beam energy, the beam spot size and the distance from the point source (Kry et al., 2007). These parameters were adjusted according to the measured dose profiles and PDD curves. Since the main interest in our study was the neutron contamination, for the purpose of our work, the accuracy of the PDD curves and beam profiles was not essential. Thus, we decided that 3% discrepancy from measurements is acceptable in the high dose region and 20% in the low dose region. Recommended values for commissioning of photon beams are 2% and 20% respectively (Ongaro et al., 2000). The energy of the primary electron beam was found to be 18 MeV. It was adjusted according to the measured PDD curves. The size of FWHM of the electron beam was set to be 0.14 cm according to the measured photon profiles. The secondary collimator (jaws) were opened to fit six different fields: 40×40, 20×20, 10×10, 5×5, 2×2 and 0×0 (all in cm^2) to investigate the effect of the jaws on the neutron flux. Small fields were of our particular interest since these fields are typically used in modern radiotherapy and especially in IMRT treatments so the beams were tuned to be as accurate as possible for small field sizes and leaving more discrepancies in large field sizes.

As mentioned before, we simulated the LINAC's 18 MV photon beams and correlated them with measured data to tune the model. Water phantom with dimensions of 60 cm $\times$ 60 cm and a depth of 50 cm was constructed, and series of cells to measure PDDs and dose profiles were constructed in the phantom. Cells used to measure PDDs had dimensions of 1 cm $\times$ 1 cm $\times$ 0.25 cm, resulting in volume of 0.25 cm^3. These cells were set one after another for the first 5 cm, and after that the space between each cell was 0.75 cm, up to 40 cm of water phantom depth, resulting in overall 55 cells for PDD estimation. To estimate dose profiles, arrays of cells were set up at depths of 3 and 10 cm. Both in-plane and cross-plane profiles were estimated. These cells had dimensions of 0.5 cm $\times$ 0.5 cm $\times$ 1 cm (volume of 0.25 cm^3). Each array consisted

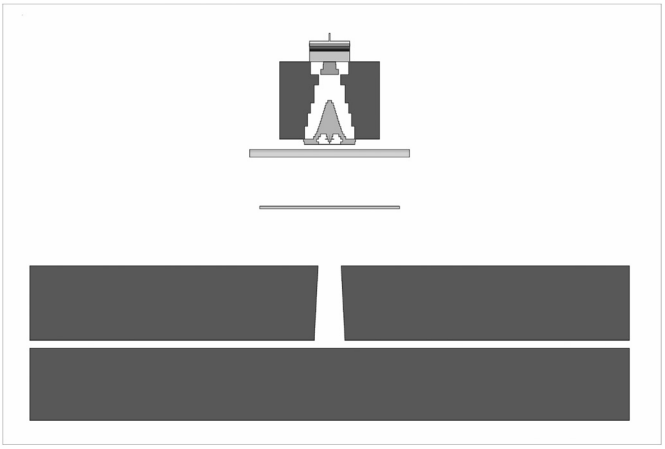

Fig. 1. Cross section model of Siemens Oncor linear accelerator head along with 18 MV beam flattening filter.

of 98 of these cells. Both PDD curves and dose profiles were estimated using F6 tally defined in MCNP611 code. The final model of photon beam consisted of 583 cells and 414 surfaces. However, for the 2×2 cm^2 field smaller detectors were used; their width was 0.1 cm, other dimensions unchanged and overall volume was 0.05 cm^3.

For each opening of the jaws, a separate simulation was conducted. Each simulation had at least 7×10^8 initial events (electrons incident on target). All particles crossing plane at 40 cm from the source (right below the jaws) were collected in a separate phase-space file. Neutron and photon dose profiles have been calculated by repeatedly feeding back the particles from the phase space till the R values for all the tallies fell below 0.1 (0.05 in case of photons).

3. Results

At first, we tuned our model according to the measured photon data. Measured and MC calculated PDD data for field sizes 40×40 cm^2, 20×20 cm^2, 10×10 cm^2, 5×5 cm^2 and 2×2 cm^2 are shown in the Fig. 2. For all field sizes, measured and calculated data show agreement better than 2% in high dose region, what is found to be satisfactory (Kry et al., 2007; Ongaro et al., 2000).

Calculated and measured dose profiles (inplane) at 10 cm depth for fields 40×40 cm^2, 20×20 cm^2, 10×10 cm^2, 5×5 cm^2 and 2×2 cm^2 are shown in the Fig. 3. Though all profiles met previously set criteria, we concentrated more on smaller field sizes since those are the field sizes mostly used in modern radiotherapy techniques. Nevertheless, for all field sizes, measured and calculated data show agreement better than 3% in the high dose region.

When we assured that the model of the accelerator complies well with the measured photon data, we used it to analyze the neutron flux in the patient plane of LINAC. First we calculated the neutron source strength (Q) defined as a number of neutrons coming from the head of the treatment unit per x-ray dose (Gy) delivered at the isocenter (NCRP60, 1984). The source strength was found to be 1.12×10^{12} neutrons per photon Gy at the isocenter, what is comparable to results found before (Chibani and Ma, 2003; Followill et al., 2003; Zabihinpoor and Hasheminia, 2011).

After validation of the model we analyzed the change in the neutron flux at the isocenter when different photon beam field sizes are used. The results are presented in the Table 1. Also, the changes in the dose equivalent and the neutron-to-photon dose equivalent ratio in the isocenter are presented. For both neutron and photon doses a $2 \times 2 \times 1$ cm^3 cell was placed at the isocenter and F4 tally was used. The corresponding neutron dose equivalent was determined by using ICRP 74 (ICRP, 1996) conversion factors. The data for the completely closed jaws are shown only for the neutron flux and the neutron dose equivalent, since photon flux, dose and neutron to photon flux ratio do not have any clinical importance.

The dependence of the neutron flux on the off-axis distance is shown in the Fig. 4. Neutron profiles are detected in $3 \times 3 \times 1$ cm^3 cells, placed in 10 cm distance from each other in both directions from the isocenter. The F4 tally was used to estimate the neutron flux.

We also examined the origin of neutrons at the isocenter and the 50 cm off-axis in the patient plane. In the Fig. 5, origin of neutron flux in the chosen points and for different field sizes are shown. Neutrons were categorized according to their place of origin.

The mean energy change for all calculation points is presented in the Table 2.

It can be seen that the energy change with field size is the largest at the isocenter and less pronounced when the simulation point is far from the isocenter in the patient plane. This is consistent with the Fig. 5 where the largest change of a photoneutrons source with the field size is found to be at the isocenter position. Data of the mean energy calculated at the isocenter (Table 2) are consistent with the previously published results (Chibani and Ma, 2003).

Knowing the neutron energy is important for the neutron flux to neutron dose equivalent conversion. For example, the change in neutron energy for 0×0 cm^2 and 20×20 cm^2 beam size in the isocenter is presented in the Fig. 6. The shift to higher neutron energies as well as higher neutron flux is present when the jaws are opened.

The energy change shown in the Fig. 6 will lead to the difference between the flux and the dose equivalent shown in the Fig. 7. Again, conversion factors from flux to the neutron dose equivalent according to the ICRP 74 (ICRP, 1996) are used.

The Fig. 7 shows that if we do not take into account the energy change in dose equivalent measurements in the isocenter when different filed sizes are used, we will introduce uncertainty up to

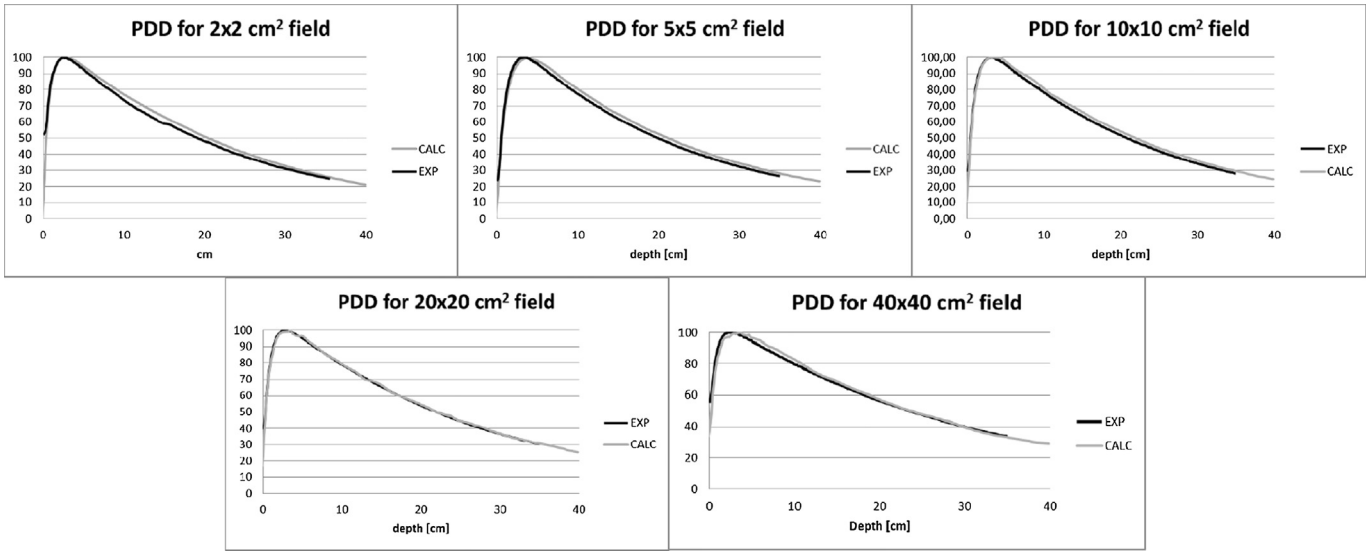

Fig. 2. Calculated and measured PDD curves. Grey line represents calculated and black line measured data.

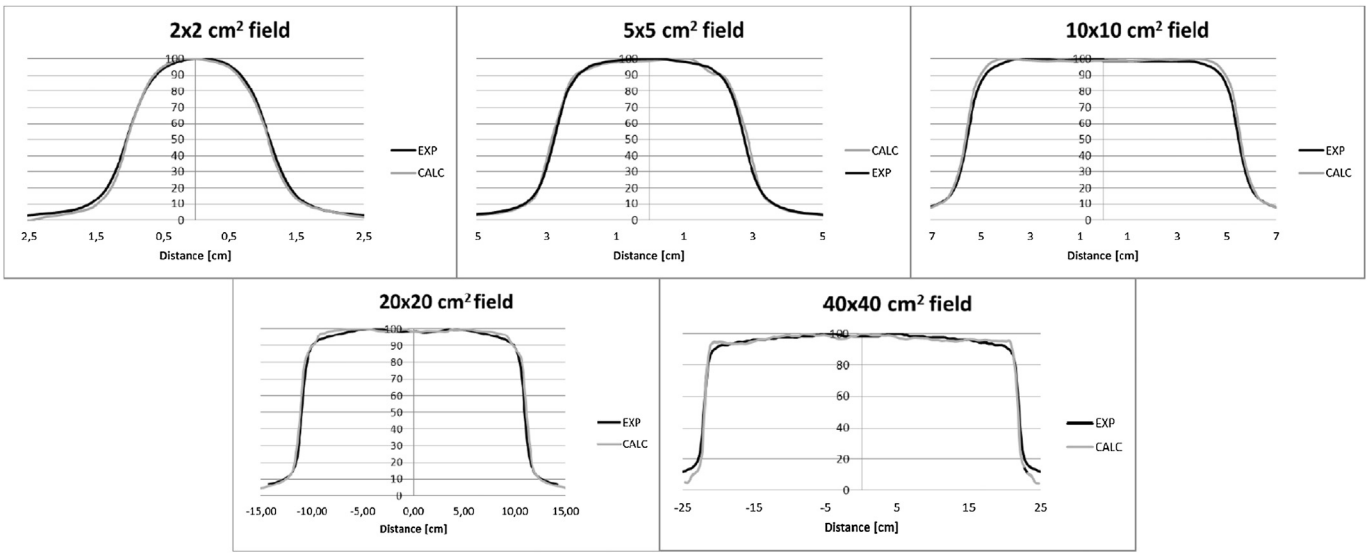

Fig. 3. Dose profiles at depth of 10 cm. Grey line presents calculated data, and black line measured data.

Table 1
Calculated neutron and photon flux and dose equivalents for different field sizes. Units for flux are particles cm^{-2}/source particle and photon and neutron dose equivalents are in Sv h^{-1}/source particle. In the last row neutron dose equivalent in mSv per photon Gy at isocenter is given.

Field size (cm^2)	0×0	2×2	5×5	10×10	20×20	40×40
Neutron flux	3.00×10^{-9}	3.72×10^{-9}	7.06×10^{-9}	8.59×10^{-9}	1.06×10^{-8}	7.48×10^{-9}
Photon flux		6.52×10^{-5}	6.88×10^{-5}	7.42×10^{-5}	7.81×10^{-5}	7.88×10^{-5}
Neutron dose equivalent	1.56×10^{-15}	3.19×10^{-15}	6.71×10^{-15}	8.82×10^{-15}	1.12×10^{-14}	8.70×10^{-15}
Photon dose equivalent		3.46×10^{-12}	3.57×10^{-12}	3.72×10^{-12}	3.81×10^{-12}	3.82×10^{-12}
Ratio (mSv/Gy)		0.9	1.9	2.4	2.9	2.3

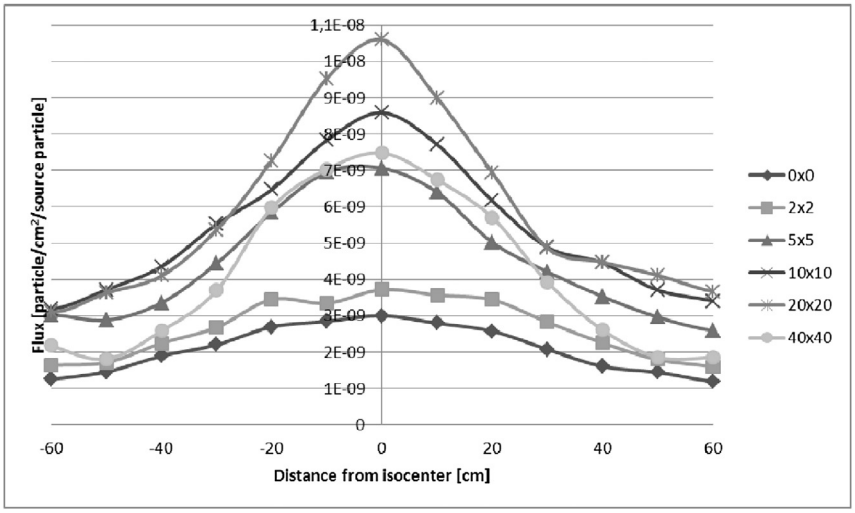

Fig. 4. Neutron flux profiles for all simulated field sizes, flux is normalized per source particle.

20% into the measurements. This will be less pronounced if we choose a point of measurement far from the isocenter in the patient plane (Table 2). Also, if we change only position in the patient plane, using the same field size, measurement uncertainty approaches 10% if we neglect neutron energy change (for 20×20 cm^2 field).

4. Discussion

The MC simulation of Siemens Oncor 18 MV photon beams and associated neutron contamination is presented in this paper. Since we calculated neutron contamination of photon beams, the accuracy of photon beam profiles and PDD curves was not essential. We accepted 3% discrepancy from measurements in the high dose region and 20% in the low dose region. The recommended values for photon beam commissioning are 2% and 20% respectively (Jurkovic et al., 2011; Kry et al., 2007; Verhaegen and Seuntjens, 2003). We achieved this accuracy for small field sizes that are more important in modern radiotherapy (Figs. 2 and 3). Neutron strength is found to

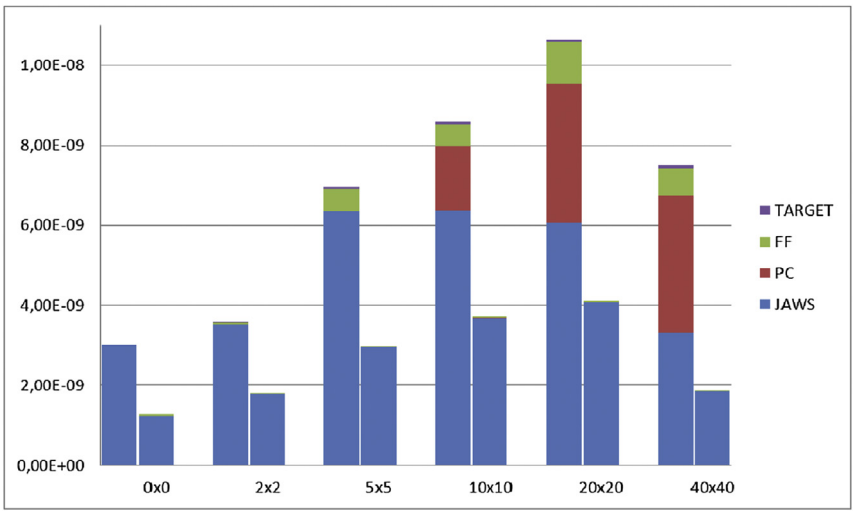

Fig. 5. Neutron flux, with neutron place-of-origin for points at IC and 50 of axes are shown. Flux at IC is higher and change of neutrons' origin gets larger as secondary collimators open.

Table 2
Mean energies of both measuring points and all field sizes in MeV are shown.

Field size (cm^2)	Of axis distance (cm)	
	50	0
0 × 0	0.31	0.21
2 × 2	0.35	0.16
5 × 5	0.34	0.40
10 × 10	0.41	0.58
20 × 20	0.49	0.71
40 × 40	0.45	0.63

because of high dose-conformity demands. Consequently, this makes neutron flux determination even more important as shown in following estimation:

According to the Table 1, neutron dose equivalent lies between 1 and 3 mSv per photon Gy at isocenter. It is easy to calculate that the total neutron dose equivalent for the complete treatment of 60 Gy photon dose lies between 60 and 180 mSv. If we take into the account that in modern radiotherapy techniques number of MU delivered for 1 photon Gy is 2–6 times higher than in conventional treatment (Quan et al., 2012) it would also mean that neutron dose

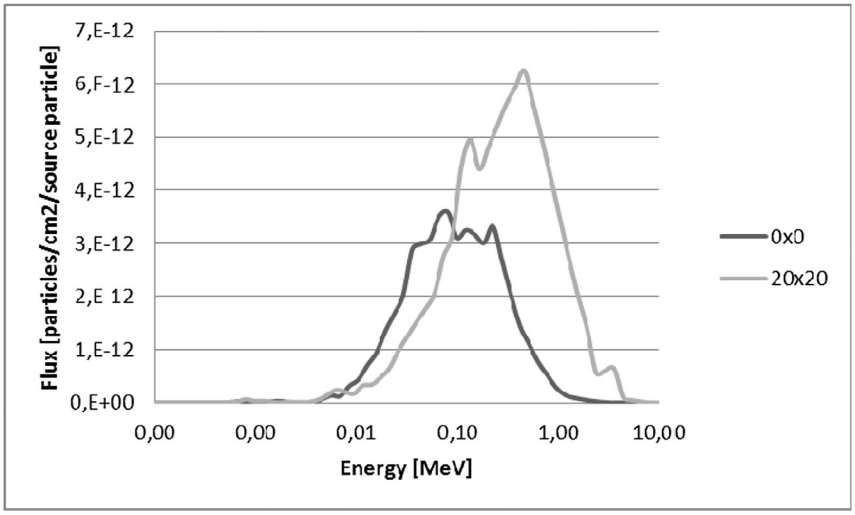

Fig. 6. Change in energy flux and spectra between 0 × 0 cm^2 and 20 × 20 cm^2 at isocenter.

be 1.12 × 10^{12} neutrons per photon Gy at the isocenter and it complies well with the published data (Chibani and Ma, 2003; Followill et al., 2003; Zabihinpoor and Hasheminia, 2011).

Change of the field size has small effect on the shape of the neutron flux (Fig. 4) as showed previously (Chibani and Ma, 2003). According to this, it is reasonable to conclude that the neutron dose equivalent to the patient is proportional to the photon beam-on time. Beam-on time is much higher in the modern radiotherapy equivalent for typical treatment could reach higher values and represent a significant risk for healthy tissues and contribute to secondary malignance.

The neutron flux dependence on the field size is showed in the Table 1 and it can also be seen in the Fig. 5. The neutron flux in the IC is increasing with the field size until maximum is reached at 20 × 20 cm^2, as already showed (Krmar et al., 2012). This is also true for the point in the patient plane 50 cm off-axis (Fig. 5). The

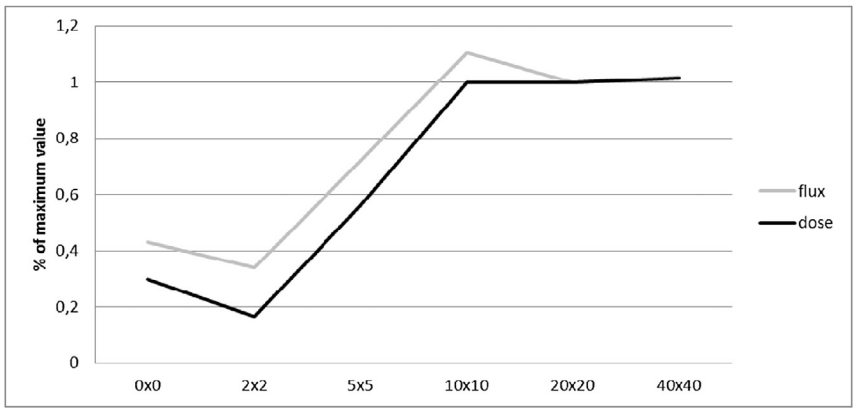

Fig. 7. Neutron flux and dose equivalent normalized at the highest values for different beam sizes.

reasonable assumption is that the most of neutrons come from the top of the LINAC head and are being attenuated by the secondary collimator. Since the neutron flux decreased at 40 × 40 cm^2, it is also reasonable to assume that besides attenuation of the neutron flux, the jaws are also source of photoneutrons (both attenuation and amplification of neutron flux by the jaws are present). To confirm and analyze this, we checked the origin of neutrons coming to the patient plane (Fig. 5) for different photon field sizes.

Opening of the secondary collimator results in more neutrons which originate from the flattening filter and the primary collimator (Fig. 5), what complies with previously published results (Chen et al., 2006; Chibani and Ma, 2003; Naseri and Mesbahi, 2010). The energy distribution of neutrons emitted by photonuclear process has two components: a peak around 1 MeV due to nuclear evaporation and a bump in the higher region due to direct reaction. Also, neutron angular distribution is assumed to be isotropic, since direct neutrons characterized by a $\sin^2 \alpha$ angular distribution (α is an angle between photon and neutron directions) represent only around 10% of the entire spectrum, while neutrons generated by evaporative process are isotropically emitted (Ongaro et al., 2000). Nevertheless, it can be expected that larger percent of direct neutrons (with higher energy) will reach the patient plane because they are more directed forward, toward the isocenter. Also, it is expected that neutrons originating from the parts of photon beam collimating system made of tungsten will have less energy comparing to the neutrons originating from iron or steel parts since the energy threshold for photonuclear reaction in tungsten is lower. This means that neutron energy will be higher if neutrons from the upper parts of the accelerator head reach the patient plane, especially if they originate from the flattening filter. Neutron contributions from LINAC head components in the isocenter change with field sizes (Fig. 5). In fact, the larger the field size, the more neutrons come from the primary collimator and the flattening filter. It explains higher mean energy for larger field sizes (Table 2). This is much less pronounced at 50 cm off-axis since the major part of neutrons originates from the jaws in all field sizes.

Data from the Fig. 5 also show that the target is not relevant source of neutron contamination, what is explained with significantly lower cross section of (e, n) reaction in comparison to photonuclear reactions in materials used in the accelerator head.

It is well known that the main limitation of most neutron detectors is energy dependence. We show that in the patient plane there is a significant energy shift when the photon beam field size is changed (Table 2). The largest difference in neutron energy spectra is shown in the Fig. 6. If we do not take this into account when making conversion from neutron flux to neutron dose equivalent, it will lead up to 20% error just by changing the field size (Fig. 7). Also, the energy change caused by the change of the measurement point in the patient plane will introduce uncertainty in measurements above 10% in some cases (20 × 20 cm^2 field size).

The energy change becomes even more important if neutron dose equivalent is measured by detector using ^{10}B as converter as e.g. in nuclear track detectors CR39. There, the layer of ^{10}B converts neutron flux into the alpha particles by (n, alpha) process (Poje et al., 2014; Sykora et al., 2007; Vukovic et al., 2010) and cross section for (n, alpha) of ^{10}B have large energy dependence. So especially in these cases, the energy change in the patient plane should not be neglected.

To conclude, if neutron detectors are used without taking into account shown energy change, a significant uncertainty would be introduced in the measurements in the patient plane. In the next future we will also consider the LINAC room in the simulation to account for energy change in the neutron flux when neutrons are scattered from the barriers surrounding LINAC to the patient plane.

Acknowledgements

This work was supported by ESF HR.3.2.01–0283 project.

References

Becker, J., Brunckhorst, E., Schmidt, R., 2008. Investigation of the neutron contamination in IMRT deliveries with a paired magnesium and boron coated magnesium ionization chamber system. Radiother. Oncol. 86, 182–186.
Chen, C., Sheu, R., Yeh, C., Lin, U., Jiang, S., 2006. A detailed study on the neutron contamination for a 10MeV medical electron accelerator. Nucl. Instrum. methods Phys. Res. Sect. A Accel. Spectrom. Detect. Assoc. Equip. 562, 1033–1037.
Chibani, O., Ma, C.-M.C., 2003. Photonuclear dose calculations for high-energy photon beams from Siemens and Varian linacs. Med. Phys. 30, 1990–2000.
Cox, L.J., Casswell, L., 2014. MCNP (TM) Release 6.1. 1 Beta: Creating and Testing the Code Distribution. Los Alamos National Laboratory (LANL).
Donadille, L., Trompier, F., Robbes, I., Derreumaux, S., Mantione, J., Asselineau, B., Amgarou, K., Martin, A., Bottollier-Depois, J., Queinnec, F., 2008. Radiation protection of workers associated with secondary neutrons produced by medical linear accelerators. Radiat. Meas. 43, 939–943.
Followill, D.S., Stovall, M.S., Kry, S.F., Ibbott, G.S., 2003. Neutron source strength measurements for Varian, Siemens, Elekta, and general electric linear accelerators. J. Appl. Clin. Med. Phys. 4, 189–194.
Howell, R.M., Ferenci, M.S., Hertel, N.E., Fullerton, G.D., 2005. Investigation of secondary neutron dose for 18MV dynamic MLC IMRT delivery. Med. Phys. N. Y. Inst. Phys. 32, 786–793.
ICRP, 1996. Conversion coefficients for use in radiological protection against external radiation. Ann. ICRP 26, 3–4.
Jabbari, K., Anvar, H.S., Tavakoli, M.B., Amouheidari, A., 2013. Monte carlo simulation of siemens oncor linear accelerator with beamnrc and dosxyZnrc code. J. Med. signals sensors 3, 172.
Jahangiri, M., Hejazi, P., Hashemi, S.M., Haghparast, A., Hajizadeh, B., 2015. The effect of field size and distance from the field center on neutron contamination in

medical linear accelerator. Int. J. Adv. Biol. Biomed. Res. 3, 97–104.
Jurkovic, S., Zauhar, G., Faj, D., Radojcic, D., Svabic, M., Kasabasic, M., Diklic, A., 2011. Dosimetric verification of compensated beams using radiographic film. Radiol. Oncol. 45, 310–314.
Krmar, M., Baucal, M., Božić, N., Jovančević, N., Ciraj-Bjelac, O., 2012. Neutron dose equivalent measured at the maze door with various openings for the jaws and MLC. Med. Phys. 39, 1278–1281.
Kry, S.F., Salehpour, M., Followill, D.S., Stovall, M., Kuban, D.A., White, R.A., Rosen, I.I., 2005. Out-of-field photon and neutron dose equivalents from step-and-shoot intensity-modulated radiation therapy. Int. J. Radiat. Oncol. Biol. Phys. 62, 1204–1216.
Kry, S.F., Titt, U., Followill, D., Pönisch, F., Vassiliev, O.N., White, R.A., Stovall, M., Salehpour, M., 2007. A Monte Carlo model for out-of-field dose calculation from high-energy photon therapy. Med. Phys. 34, 3489–3499.
McGinley, P., Wood, M., Mills, M., Rodriguez, R., 1976. Dose levels due to neutrons in the vicinity of high-energy medical accelerators. Med. Phys. 3, 397–402.
Naseri, A., Mesbahi, A., 2010. A review on photoneutrons characteristics in radiation therapy with high-energy photon beams. Rep. Pract. Oncol. Radiother. 15, 138–144.
NCRP60, 1984. Neutron Contamination from Medical Electron Accelerators: Recommendations of the National Council on Radiation Protection and Measurements. Ncrp Report 60, Bethesda, MD, USA.
Ongaro, C., Zanini, A., Nastasi, U., Ródenas, J., Ottaviano, G., Manfredotti, C., 2000. Analysis of photoneutron spectra produced in medical accelerators. Phys. Med. Biol. 45, L55.
Poje, M., Ivkovic, A., Jurkovic, S., Zauhar, G., Vukovic, B., Radolic, V., Miklavcic, I., Kaliman, Z., Planinic, J., Brkic, H., Faj, D., 2014. The neutron dose equivalent around high energy medical electron linear accelerators. Nucl. Technol. Radiat. Prot. 29, 207–212.
Quan, E.M., Li, X., Li, Y., Wang, X., Kudchadker, R.J., Johnson, J.L., Kuban, D.A., Lee, A.K., Zhang, X., 2012. A comprehensive comparison of IMRT and VMAT plan quality for prostate cancer treatment. Int. J. Radiat. Oncol. Biol. Phys. 83, 1169–1178.
Schraube, H., Kneschaurek, P., Schraube, G., Wagner, F., Weitzenegger, E., 2002. Neutron spectra around medical treatment facilities. Nucl. Instrum. Methods Phys. Res. Sect. A Accel. Spectrom. Detect. Assoc. Equip. 476, 463–467.
Sykora, G.J., Akselrod, M.S., Salasky, M., Marino, S.A., 2007. Novel Al2O3: C, Mg fluorescent nuclear track detectors for passive neutron dosimetry. Radiat. Prot. Dosim. 126, 278–283.
Verhaegen, F., Seuntjens, J., 2003. Monte Carlo modelling of external radiotherapy photon beams. Phys. Med. Biol. 48, R107.
Vukovic, B., Faj, D., Poje, M., Varga, M., Radolic, V., Miklavcic, I., Ivkovic, A., Planinic, J., 2010. A neutron track etch detector for electron linear accelerators in radiotherapy. Radiol. Oncol. 44, 62–66.
Zabihinpoor, S., Hasheminia, M., 2011. Calculation of neutron contamination from medical linear accelerator in treatment room. Adv. Stud. Theor. Phys. 5, 421–428.
Zanini, A., Durisi, E., Fasolo, F., Ongaro, C., Visca, L., Nastasi, U., Burn, K., Scielzo, G., Adler, J.-O., Annand, J., 2004. Monte Carlo simulation of the photoneutron field in linac radiotherapy treatments with different collimation systems. Phys. Med. Biol. 49, 571.